

# Checkpoint-apoptosis uncoupling in human and mouse embryonic stem cells: a source of karyotypic instability

Charlie Mantel,<sup>1</sup> Ying Guo,<sup>1</sup> Man Ryul Lee,<sup>4</sup> Min-Kyoung Kim,<sup>2</sup> Myung-Kwan Han,<sup>1</sup> Hirohiko Shibayama,<sup>3</sup> Seiji Fukuda,<sup>1</sup> Mervin C. Yoder,<sup>1</sup> Louis M. Pelus,<sup>1</sup> Kye-Seong Kim,<sup>4</sup> and Hal E. Broxmeyer<sup>1</sup>

<sup>1</sup>Department of Microbiology & Immunology and the Walther Oncology Center, Indiana University School of Medicine, and the Walther Cancer Institute, Indianapolis, IN; <sup>2</sup>Department of Medical Genetics, Hanyang University College of Medicine, Seoul, South Korea; <sup>3</sup>Department of Hematology and Oncology, Osaka University Graduate School of Medicine, Japan; <sup>4</sup>Department of Anatomy and Cell Biology, Hanyang University College of Medicine, Seoul, South Korea

**Karyotypic abnormalities in cultured embryonic stem cells (ESCs), especially near-diploid aneuploidy, are potential obstacles to ESC use in regenerative medicine. Events causing chromosomal abnormalities in ESCs may be related to events in tumor cells causing chromosomal instability (CIN) in human disease. However, the underlying mechanisms are unknown. Using multiparametric permeabilized-cell flow cytometric analysis, we found that the mitotic-spindle checkpoint, which helps maintain chromo-**

**somal integrity during all cell divisions, functions in human and mouse ESCs, but does not initiate apoptosis as it does in somatic cells. This allows an unusual tolerance to polyploidy resulting from failed mitosis, which is common in rapidly proliferating cell populations and which is reduced to near-diploid aneuploidy, which is also common in human neoplastic disease. Checkpoint activation in ESC-derived early-differentiated cells results in robust apoptosis without polyploidy/aneuploidy similar to that in**

**somatic cells. Thus, the spindle checkpoint is “uncoupled” from apoptosis in ESCs and is a likely source of karyotypic abnormalities. This natural behavior of ESCs to tolerate/survive varying degrees of ploidy change could complicate genome-reprogramming studies and stem-cell plasticity studies, but could also reveal clues about the mechanisms of CIN in human tumors. (Blood. 2007;109:4518-4527)**

© 2007 by The American Society of Hematology

## Introduction

An important task facing living organisms from birth to death is maintenance of the genome and its transfer to offspring. Elaborate mechanisms have developed to detect, repair, and prevent transfer of genome damage.<sup>1,2</sup> Mechanisms such as DNA repair or apoptotic culling of damaged cells have been evolutionarily conserved from the simplest multicellular organisms. Genome maintenance is especially important in cells of developing mammalian embryos deriving from a single zygotic cell and in adult stem cells, such as hematopoietic stem cells. A particularly vulnerable time in the life of eutherian mammals is the time from fertilization through cleavage and blastocyst formation, prior to uterine implantation, where developing embryos must survive almost independent from maternal nurturing. A highly specialized program of cellular regulation operates during this time, especially in pluripotent embryonic stem cells (ESCs) derived from the blastocyst that give rise to all adult somatic tissues.<sup>3-11</sup> ESCs from several mammalian species, including humans, isolated and cultured in vitro as immortalized cell lines,<sup>12,13</sup> provide the potential for therapeutic use in humans. Understanding these specialized embryonic strategies of genome maintenance is necessary to ensure their safe and effective use and may also reveal clues for studies of potentially similar behavior in adult stem cells.

Immortalized mouse (m) and human (h) ESCs are subject to genetic and epigenetic instability, primarily chromosomal aberrations such as loss of heterozygosity, uniparental disomy, and aneuploidy.<sup>14-21</sup> This increases the risk of tumorigenic potential and

other complications if hESCs are to be used therapeutically. Such behavior is likely related to their specialized strategies for genome maintenance, such as truncated cell cycles with very short or absent gap phases and differences in certain cell-cycle checkpoints compared with somatic cells.<sup>2-5</sup> A problem with analyzing protein biochemistry of ESCs using conventional techniques such as gel electrophoresis/immunoblotting is that changes in protein content in small but distinct populations such as those cells in M phase of the cell cycle, or in subpopulations of heterogeneous ESC colonies, might be masked when large numbers of cells are used for protein extraction. We have overcome this problem by using permeabilized-cell flow cytometry techniques that can quantitate proteins in individual cells where their precise cell-cycle states or developmental marker statuses can be simultaneously determined. This also has an advantage over immunocytochemical techniques because large numbers of cells can be analyzed quickly. Using this approach, we now report in mESCs, and for the first time in hESCs, that the mitotic spindle assembly checkpoint (SAC) is functional, but fails to prevent rereplication and polyploidy after drug-induced spindle microtubule disruption and SAC activation or after DNA double-strand breaks. We demonstrate that h/mESCs, which do have the molecular machinery for apoptosis, have a remarkable tolerance for mitotic failure-induced polyploidy, a condition rarely observed in most mammalian somatic cells. Polyploid ESC mitotic cell divisions (4C-8C-4C) also occur for brief periods in culture, but upon

Submitted October 25, 2006; accepted January 23, 2007. Prepublished online as *Blood* First Edition Paper, February 8, 2007; DOI 10.1182/blood-2006-10-054247.

The online version of this manuscript contains a data supplement.

The publication costs of this article were defrayed in part by page charge payment. Therefore, and solely to indicate this fact, this article is hereby marked “advertisement” in accordance with 18 USC section 1734.

© 2007 by The American Society of Hematology

induced differentiation, preformed and isolated polyploid/aneuploid ESCs initiate caspase-dependent apoptosis. This indicates that switching from pluripotency to lineage specification activates silenced cell-death checkpoint-coupling programs. We suggest that ESCs display intrinsic absence of checkpoint-apoptosis coupling. Because the SAC is crucial during every cell division and because mitotic errors often occur in rapidly proliferating cell populations, this coupling is important for genome maintenance. Therefore, uncoupling can contribute to karyotypic abnormalities seen in ESCs cultured *in vitro*, which is an obstacle that must be overcome for their safe use in therapeutic applications in humans.

## Materials and methods

### Cells, cell lines, and culture methods

mESC lines E14, R1, CCE, and JSR were cultured as described<sup>22,23</sup> on primary mouse embryonic fibroblast (MEF) feeder layers after MEF inactivation by  $\gamma$  irradiation, and transferred to gelatin-coated dishes for experiments. Initial passage number for all mESC lines was between 6 and 10, and new cultures were started from frozen stocks after the 20th passage. The hESC line MI01 (MIZ-hES1) was obtained from MizMedi Women's Hospital (Seoul, Korea) at passage number 56, and new cultures were started after passage 80. The MI01 cell line has a karyotype of 46, XY, and its characterization can be found online at the National Institutes of Health (NIH) Human Stem Cell Registry.<sup>24</sup> MI01 was cultured as described<sup>25,26</sup> on mitomycin-C-inactivated MEF feeder layers using manual colony microdissection.<sup>26</sup> This method was also used for harvesting cells for experiments, and single-cell suspensions were prepared using 0.05 M EDTA.<sup>25</sup> Shortly after these studies were done, it was revealed by the Korean government that MI01 (MIZ-hES1) was, in fact, the MIZ-hES5 cell line. This hESC line is 46X,Y, and its further characterization can be obtained from MizMedi Women's Hospital. The mouse growth-factor-dependent pro-B-lymphocyte parental cell line Ba/F3 was maintained as reported.<sup>27-29</sup> The anamorsin-overexpressing Ba/F3 cell line and empty vector control cells were maintained as we reported.<sup>28</sup> Human growth-factor-dependent MO7e cells were maintained in culture as we reported.<sup>27,30</sup> Ba/F3 cells overexpressing survivin were maintained as reported.<sup>29</sup>

### Antibodies, cytokines, and drugs

FITC-labeled antibody to active (cleaved) caspase-3, and isotype-matched control antibodies, FITC-labeled annexin-V, and propidium iodide were obtained from BD Biosciences Pharmingen (San Diego, CA). Other antibodies and their isotype controls were from Cell Signaling Technology (Beverly, MA). LIF, interleukin-3, and other cytokines were obtained from R&D Systems (Minneapolis, MN). Nocodazole, paclitaxel, retinoic acid, and Wright-Giemsa were from Sigma Chemical (St Louis, MO). Etoposide was from Bristol-Meyers Squibb Oncology (Princeton, NJ). Drugs were dissolved and diluted either in ethanol or DMSO. Treatments with nocodazole, paclitaxel, or etoposide were done as we reported.<sup>27,30</sup> For nocodazole treatment of hESC colonies, a dose-response experiment was performed (Figure S5, available on the *Blood* website; see the Supplemental Materials link at the top of the online article). A concentration of 0.05  $\mu$ g/mL was selected for all other experiments.

### Multivariate permeabilized-cell flow cytometry and cell-cycle analysis

After harvest and washing with PBS, single-cell suspensions were permeabilized and fixed using Cytofix/Cytoperm (BD Biosciences Pharmingen), stained with various labeled antibodies, and washed and counterstained with propidium iodide.<sup>27,30</sup> Flow cytometric data were acquired with FACScan, FACSCaliber II, or FACS Vantage flow cytometers using CellQuest software for initial compensation (BD Biosciences Pharmingen). Relative fluorescence intensity histograms and dot-plots of data were made and analyzed with WinList 5.0 and ModFit 3.0 programs from Verity

Software House (Topsham, MA). Postacquisition compensation and hyperlog transformation<sup>31</sup> were applied with the WinList 5.0 program. Cell permeabilization, fixation, staining, and data acquisition for all samples were done on the same day, using the same instrument for each individual experiment for consistency. Tests for statistical significance among independent experiments were done with the Student *t* test.

### Chromosome counting and photomicroscopy

After harvest and washing, cells fixed with a methanol-acetic acid mixture, and metaphase chromosome spreads were prepared as per Henegariu et al<sup>32,33</sup> and online (<http://info.med.yale.edu/genetics/ward/tavi/FISH.html>). Chromosomes were stained with Wright-Giemsa (Sigma Chemical). For cellular morphology, slides were prepared using a Hematech-1000 cytocentrifuge from Miles Diagnostics (Elkhart, IN), and cells were stained with Wright-Giemsa. Photomicroscopy for hESC colony morphology was done with an Olympus Imaging America (Center Valley, PA) SZ51 inverted microscope system, or Nikon Diaphot, or Nikon Labophot-2 compound microscope (Tokyo, Japan) was used for mESC photos. Immersion oil was from Cargille (Cedar Grove, NJ). Photomicrographs using Nikon Diaphot and Labophot-2 were taken with Nikon Coolpix-SI with SI v10 software. Photos were organized and cropped with MS Office Picture Manager software.

## Results

### mESCs exit mitosis and become polyploid after prolonged spindle checkpoint activation

To begin to understand the sources of karyotypic abnormalities during culture of ESCs, we investigated the function of the SAC. mESCs accumulate in the M phase of the cell cycle after microtubule disruption with nocodazole or paclitaxel, but also exit mitotic delay and reenter polyploid mitosis (Figure 1A-C). A total of 2 populations of mESCs with high phosphohistone H3, 1 with 4C and 1 with 8C DNA content, demonstrate transiency of the SAC. Mitotic exit with 4C DNA content does not activate processes known in normal somatic cells to initiate apoptosis or senescence.<sup>34-36</sup> This finding in 4 different mESC lines (Figures 1,S1) suggests it is a generalized response in mESCs. Metaphase chromosome counts confirmed polyploidy/aneuploidy (Figures 1D-E,S2C). Figures 1F and S2A demonstrate the chromosomes are located in a single nucleus. We refer to these as mononuclear polyploid/aneuploid (MNP). It is important to understand that normal somatic cells and cell lines with normal p53 responses do not respond to prolonged SAC activation in this way. They initiate apoptosis after exiting the cell cycle in a G<sub>0</sub>/G<sub>1</sub>-like state with 4C DNA content, often in 2 nuclei, or enter senescence.<sup>34,35</sup> MNP cells expressed the pluripotent marker SSEA-1 (Figure S2B), indicating they are undifferentiated.<sup>37</sup> We conclude that the SAC, which is essential for correct chromosome segregation in somatic cells,<sup>2</sup> is transiently functional in mESCs but fails to prevent rereplication and MNP formation. This suggests that some aspects of SAC and/or other related checkpoints (like the G<sub>1</sub> MTA/tetraploidy checkpoint<sup>30,38</sup>), are absent or silenced in ESCs compared with somatic cells.

### mESCs resist initiation of apoptosis after SAC activation and MNP cell formation

To better understand mechanisms of MNP cell formation and survival after aberrant mitotic exit, we investigated apoptotic responses of mESCs after SAC activation. mESCs are resistant to caspase-3 activation after SAC activation and MNP cell formation (Figure 2A-B). Identical experiments were also performed on

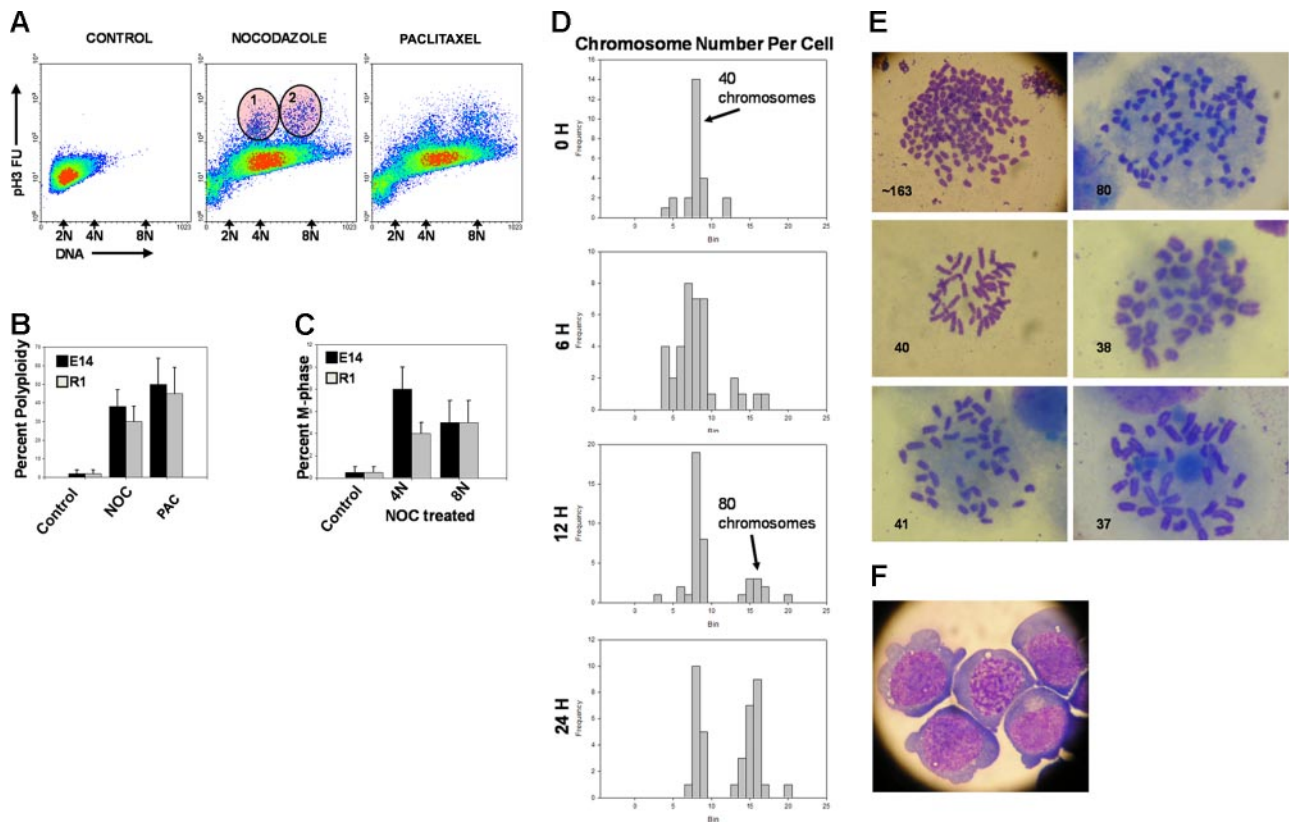


**Figure 1. Microtubule disruption-induced mitotic arrest and polyploidy in mESCs.** mESC lines E14 and R1 were treated with nocodazole (for microtubule depolymerization), paclitaxel (for microtubule overstabilization), or control solvent for 24 hours in complete culture medium containing LIF as described in "Materials and methods." (A) Cells were harvested and assayed by multivariate permeabilized-cell cell-cycle analysis for simultaneous phospho(ser10)histone-H3 and DNA content. Regions 1 and 2 indicate E14 cells that are in M phase as indicated by increased phosphohistone-H3 content at 4C and 8C DNA content) analysis in E14 and R1 cells from 6 independent experiments is shown as the mean  $\pm$  1SD. (B) Results of polyploidy (cells with  $>$  4C DNA content) analysis in E14 and R1 cells from 6 independent experiments is shown as the mean  $\pm$  1SD. (C) Percentage of M-phase cells (regions 1 and 2) are shown. (D) Relative frequency histograms of chromosome number in metaphase E14 cells treated with nocodazole for the indicated times showing an average of 40 chromosomes per cell (euploid) at 0 time and showing the increase in cells with 80 chromosomes (tetraploid) at 24 hours. Chromosome number indicates BIN number times 5. The experiment was repeated once with the E14 cell line and once with the R1 cell line with similar results. Chromosome counts in normal MEF cells are shown for comparison in Figure S2C. MEF cells had 40 chromosomes per cell. (E) Typical metaphase chromosome appearance in E14 cells before and after nocodazole treatment; the number of chromosomes is indicated (Nikon Labophot-2;  $10\times$  100; oil). (F) Wright-Giemsa stain of E14 cells harvested 24 hours after nocodazole treatment displaying a single nucleus. No E14 cells with more than 1 nucleus were observed (Nikon Labophot-2;  $10\times$  40).

differentiated mouse embryoid body (mEB) cells, which efficiently activated robust caspase-3-dependent apoptosis. Interestingly, the DNA-damaging agent etoposide (a topoisomerase II inhibitor that causes DNA double-strand breaks) induced robust caspase-3 activation in mEB cells but not in mESCs. Etoposide treatment also caused polyploidy and MNP cell formation similar to SAC activation (Figure S3). Etoposide typically induces cell-cycle arrest in somatic cells in the S phase of the cell cycle and not mitosis.<sup>27</sup> This suggests that ESCs are also resistant to apoptosis induced by double-strand breaks. Thus, several pathways of apoptosis induction are different in ESCs compared with somatic cells, suggesting this is a generalized response to different kinds of stresses *in vitro*.

It has been noted that late apoptotic cells can be active caspase-3-negative.<sup>39</sup> It is therefore likely that apoptosis may be underestimated by measurement of active caspase-3 alone. Another marker of apoptosis is the "sub-G<sub>1</sub>" population (cells with less than 2C DNA content).<sup>40</sup> Figure 2C shows that nearly all treated mEB cells are sub-G<sub>1</sub>, further demonstrating the marked difference between mESC and mEB apoptotic responses. We also investigated caspase-3-independent apoptosis by annexin-V binding (Figure 2D-E), which recognizes early apoptosis.<sup>41</sup> These results substantiate the caspase-3-dependent apoptosis results. Thus, mESCs do not initiate apoptosis (caspase-3-dependent or -independent) after

SAC activation and MNP cell formation. However, after LIF removal-induced differentiation, SAC activation or DNA damage results in robust apoptosis consistent with that seen in MEFs<sup>34,35</sup> and other somatic cells.<sup>36</sup>

#### Mouse MNP cells are tolerant to polyploidy but activate apoptosis upon differentiation

Because mESCs become polyploid after transient SAC activation while mEBs do not, and because mEBs activate apoptosis after SAC activation, we hypothesized there is a transition where polyploidy tolerance gives way to intolerance and subsequent apoptosis during transition from pluripotency to lineage specification. We investigated the stability of MNP cells in culture and effects of LIF removal-induced differentiation of MNP cells that were already formed. After nocodazole treatment and MNP formation, cells were washed free of nocodazole and recultured in LIF. After subculture and expansion for 4 to 6 passages, phosphohistone H3/cell-cycle analysis demonstrates that MNP cells underwent polyploid mitosis (4C  $\rightarrow$  8C  $\rightarrow$  4C). Polyploidy increased from 31% (after 24 hours of treatment) to 60% in 4 passages after treatment, wash, and reculture (4-pass; Figure 3A), and there was little apoptosis (Figure 3B; 4-pass). Control

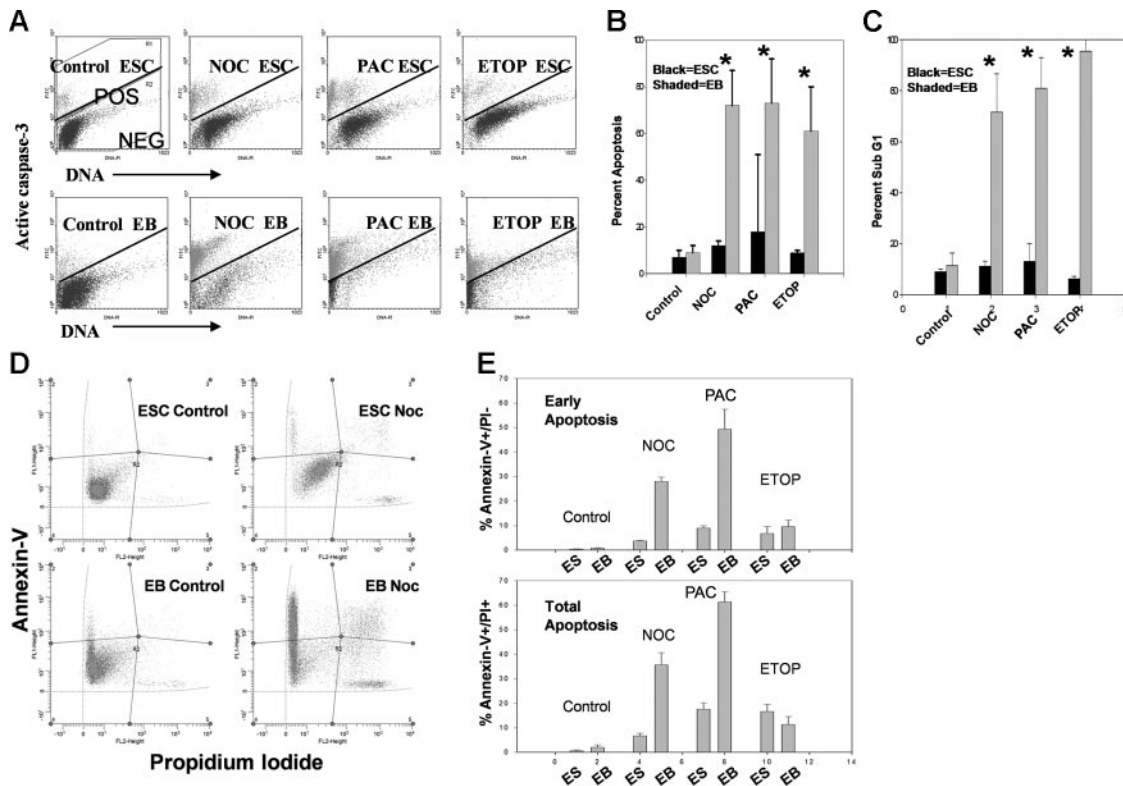


**Figure 2.** Analysis of apoptosis of E14 cells before and after treatment with microtubule-disrupting agents or after DNA damage. (A) E14 mESCs were treated with the indicated agent for 24 hours and harvested as in Figure 1. Cells were analyzed by permeabilized-cell flow cytometry as in Figure 1 except an antibody to activated caspase-3 was used. Cells above the bar are positive and those below the bar are negative for caspase-3 activation. (B) Caspase-3 activation in day-3 mEB cells after 24 hours of treatment. Percentage apoptosis (mean  $\pm$  1SD for 3 independent experiments) as indicated by caspase-3 activation. (C) Percentage apoptosis (mean  $\pm$  1SD for 3 independent experiments) as indicated by sub-G<sub>1</sub> cells. \*Statistically significant difference from control;  $P < .05$ . (D-E) Apoptosis measurement in treated and untreated mESCs or mEB cells as indicated by Annexin-V binding. Cells were simultaneously stained with propidium iodide to indicate cellular membrane integrity. Early apoptosis (Annexin-V<sup>+</sup> and PI<sup>+</sup>) and total apoptosis (Annexin-V<sup>+</sup> and PI<sup>+/−</sup>) for E14 or mEB cells before and after treatment as in panels A and B. Results are mean percentages  $\pm$  1SD for 3 independent experiments.

(untreated) cells remained 2% polyploid after wash and reculture and 1% active caspase-3–positive. The polyploidy in MNP cells decayed to near-diploid aneuploidy (indicated by DNA content), with increased caspase-3 activation when cultured beyond 4 expansion passages (Figure 3C). It is also noteworthy that the active caspase-3–negative MNP cells were primarily not sub-G<sub>1</sub>, while the active caspase-3–positive populations contained large numbers of sub-G<sub>1</sub> cells, further supporting the apoptosis analysis of MNP cells similar to that described for mESCs and mEBs (Figure 2C).

We next questioned whether pre-existing MNP cells were LIF independent or if they initiate apoptosis or differentiation upon LIF removal. Normal mESCs were placed into EB medium without LIF for 3 days. EBs formed and had about 12% apoptotic cells, which is typical for mEB formation (Figure 3D). In contrast, 4-passage MNP cells (washed free of drugs) initiated apoptosis 2 days after LIF removal and polyploidy decayed to near-diploid aneuploidy. This continued on day 3 and displayed robust caspase-3 activation without EB formation. Remarkably, active caspase-3–negative (nonapoptotic) cells remaining in the culture on day 3 were near-diploid (indicated by DNA content). We conclude that mESCs are unusually tolerant to the polyploid condition and can undergo tetraploid cell divisions in culture. Upon removal of LIF, MNP cells initiate apoptosis and do not form EBs. Also, the ploidy status of MNP cells decays after several passages, even with LIF, to become aneuploid and near-diploid within 10 to 12 passages.

### Ectopic suppression of apoptosis in 2 models of highly differentiated somatic cells results in polyploidy after SAC activation

There are 2 possible interpretations of these results of LIF removal–induced (differentiation–induced) apoptosis of MNP cells. One is intrinsic silencing of processes linking SAC to apoptosis in ESCs. We refer to this as “uncoupling.” Upon differentiation, these processes are unsilenced and activated (coupled), thus preventing MNP cell formation and survival. Another interpretation is that LIF, a known antiapoptotic cytokine,<sup>8</sup> suppresses apoptosis, allowing survival of MNP cells. This would suggest that culture conditions allow MNP cells to survive and is not due to intrinsic uncoupling. To evaluate these possibilities, we hypothesized that if MNP cell survival is due to intrinsic suppression of apoptosis, then ectopic suppression of apoptosis in a highly differentiated model somatic (coupled) cell line would also result in polyploidy after SAC activation. To test this hypothesis, we used the mouse growth-factor–dependent pro–B-lymphocyte cell line Ba/F3 and its derivative, which overexpresses the antiapoptotic protein anamorsin.<sup>28</sup> SAC activation or DNA damage–induced caspase-3–dependent apoptosis in Ba/F3 cells and anamorsin overexpression suppressed this response (Figure S4). Anamorsin-induced apoptosis suppression alone caused Ba/F3 cells to contain more than 4C DNA content. Nocodazole treatment for 48 hours caused increased polyploid (8C) cells that were not observed in treated parental Ba/F3 cultures

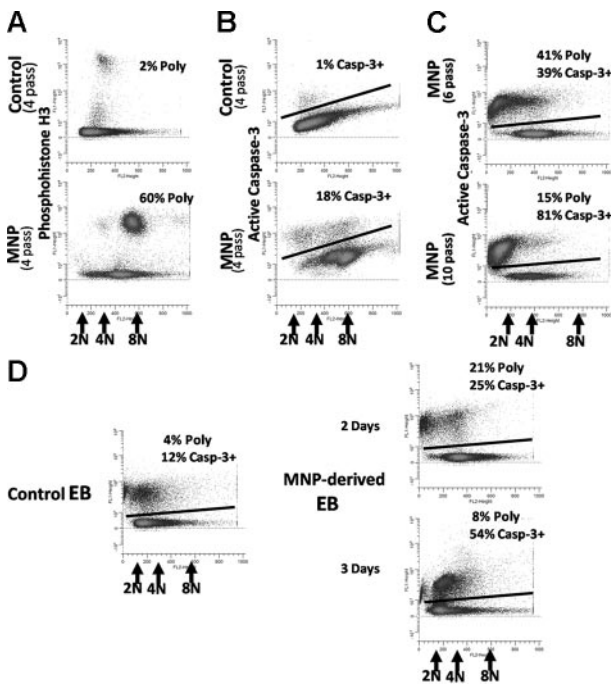


**Figure 3. Apoptosis and cell-cycle analysis in preformed mouse polyploidy ESCs and their EB formation after expansion culture.** Phosphohistone H3 (A) and caspase-3 (B) is shown in control (solvent-treated) E14 cells or in preformed polyplod (MNP) cells after cells were washed free of nocodazole or control solvent, recultured in complete medium containing LIF, and expanded by subculture for 4 passages (4-pass). They were then harvested, and multivariate cell-cycle analysis performed as in Figure 1. DNA content, percentage of polyploidy, and percentage of apoptosis are numerically indicated. (C) Apoptosis and polyploidy after 6 and 10 expansion passages of MNP is numerically shown. (D) Untreated control and MNP cells from panel A were then washed free of LIF and placed into EB medium for the indicated time, then harvested and apoptosis analysis done. DNA content and numerical percentages of polyploidy and apoptosis for untreated control cell-derived mEB cells and MNP-derived mEB cells are indicated. This experiment was repeated once with similar results.

(Figure 4A). We also investigated a Ba/F3 derivative overexpressing the antiapoptotic protein survivin (Figure 4B).<sup>29</sup> Paclitaxel-activated SAC caused polyploidy in these cells, but not in empty-vector control cells. Thus, ectopic suppression of apoptosis in 2 model somatic cell lines caused polyploidy after SAC activation, analogous to mESCs. Therefore, polyploidy can result after checkpoint activation in normally coupled somatic cells if the apoptotic machinery is deregulated, supporting the interpretation of intrinsic uncoupling in ESCs.

**Differentiation in the presence of LIF does not prevent SAC apoptosis coupling**

To further evaluate the role of LIF in MNP cell formation, we used retinoic acid (RA) to induce differentiation in mESCs while in the continued presence of LIF. Figure 4C-D demonstrates that RA treatment for 3 days causes decreased SSEA-1 expression associated with a pronounced morphology change (not shown) as already reported,<sup>37</sup> indicating they were differentiated cells (SSEA-1-Lo). After treatment with nocodazole, SSEA-1-Lo (RA-differentiated) cells failed to become polyplod, while SSEA-1-Hi (remaining undifferentiated) cells accumulated with more than 4C DNA. This suggests that even in the continued presence of LIF, differentiated mESCs will induce apoptosis (as indicated by hypodiploidy and caspase-3 activation) without tolerance for the tetraploid/polyplod condition. This also supports the hypothesis that checkpoint-apoptosis uncoupling is an intrinsic property of mESCs and not due directly to the survival effects of LIF or other culture conditions.

**hESC colonies contain 2 distinct cell types that differ in response to SAC activation, polyploidy, and pluripotent marker expression**

We next sought to extend our observations to hESCs. This also afforded us the opportunity to investigate polyploidy in the absence of exogenous LIF. hESCs do not require LIF for proliferation in vitro and were cultured on MEF feeder layers. An unexpected

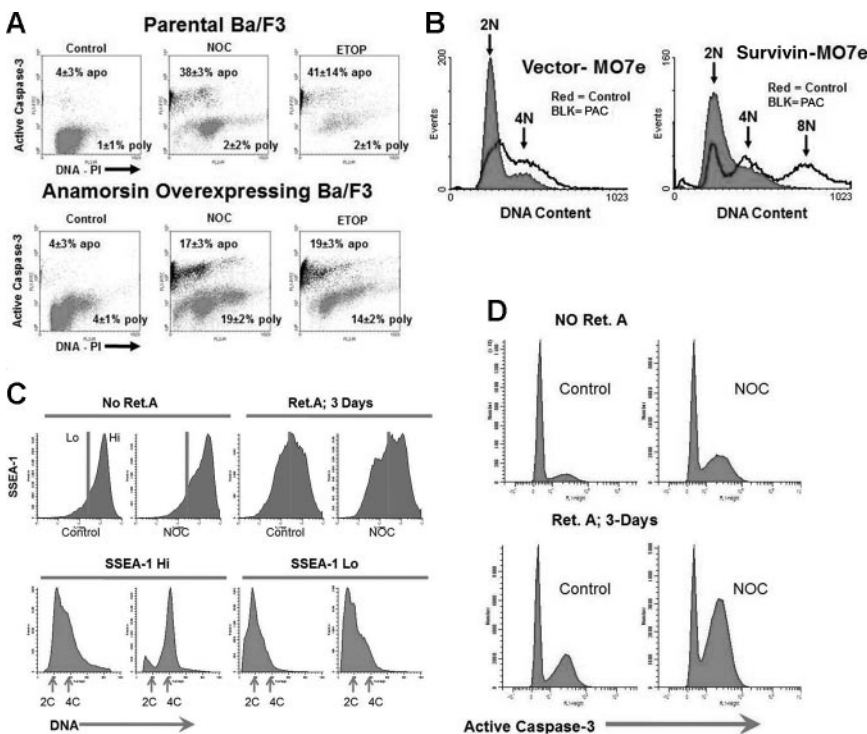


**Figure 4. Intrinsic apoptosis-suppression uncouples somatic cells, while differentiation of mESCs in the presence of LIF does not prevent coupling.** Ba/F3 cells and their derivatives containing an expression vector for overexpressing anamorsin were treated with control solvent or nocodazole or etoposide for 48 hours, then harvested and cell cycle/apoptosis analysis performed (A) as in Figure 2A. Percentages of polyploidy and apoptosis (mean ± 1SD) from 3 experiments is shown. (B) MO7e cells expressing empty vector or a vector containing survivin. Cells were treated with paclitaxel or control solvent for 48 hours then harvested, and cell-cycle analysis was performed. This experiment was repeated once with similar results. (C) E14 mESCs were treated with RA for 3 days, then treated for 1 additional day with nocodazole added. SSEA-1 expression is shown in the top panel, and cell-cycle analysis of SSEA-1-Hi and SSEA-1-Lo gated cells is shown in the bottom panel. (D) Caspase-3 activation in cultures from panel C.

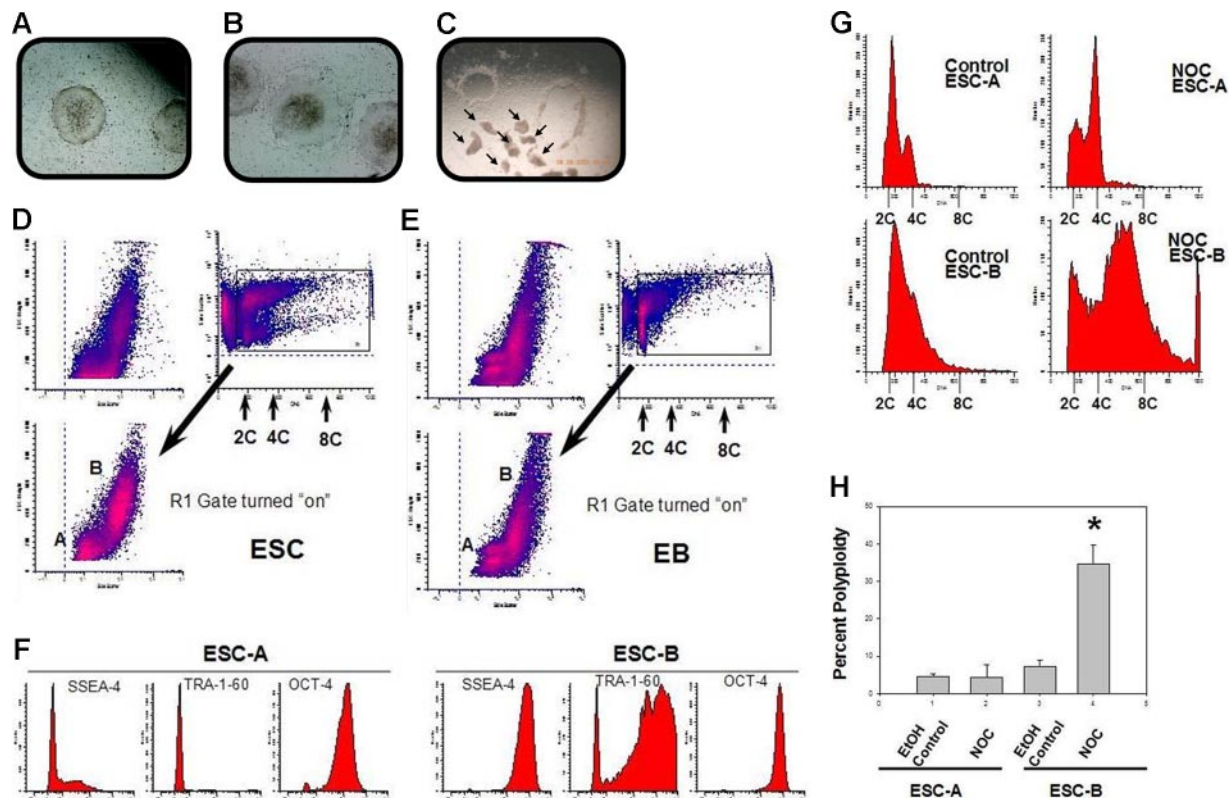


**Figure 5.** Colonies of the hESC line MI01 contain 2 cell types distinguishable by laser-light scatter patterns, expression of pluripotent markers, and ploidy in response to SAC activation. Morphology of typical (A) or atypical (B) MI01 colonies is shown. (C) Examples of microsurgical harvesting of typical colonies. Arrows indicate cut and lifted clumps of cells from colonies (Olympus S751;  $10 \times 20$ ). (D) Flow cytometric analysis of laser-light scatter pattern and DNA content was used to distinguish 2 populations, hESC-A and hESC-B, in single-cell suspensions of harvested MI01 colonies. DNA content versus laser-light side-scatter is indicated. The R1 gate was used to separate viable cells from hypodiploid cells and cell debris. The ratio of percentages of hESC-A and hESC-B cells was  $0.52 \pm 0.21$  for 6 separate experiments. Nocodazole treatment had no significant effect on this percent ( $P > .05$ ; Figure S6). MI01 colonies were harvested, washed, and placed into human EB medium and cultured for 4 days, then hEBs were harvested and single cell suspensions were analyzed (E) as in panel D. Results are representative of 2 experiments. (F) Pluripotent marker expression of hESC-A and hESC-B. Isotype control antibody-staining intensity was below 10 fluorescence units (not shown). Data are representative of 2 experiments. hESC-A and hESC-B were treated with nocodazole or control solvent as in Figure 1 and harvested. hESC-A and hESC-B cells were gated as in Figure 5D. (G) Cell-cycle analysis was performed and DNA content is shown. (H) Percentage of polyploidy (mean  $\pm$  1SD) from 3 experiments. \*Significant difference ( $P < .01$ ) for nocodazole-treated hESC-Bs compared with control hESC-Bs.

finding of 2 populations of cells in hESC colonies, with 1 being very early differentiated and the other being pluripotent (according to internal and surface-marker expression), allowed us to assess checkpoint activation simultaneously in both cell types in the same colonies. Figure 5A depicts a typical colony morphology of MI01 cells<sup>25,26</sup> cultured on mitomycin-C-inactivated MEFs with a well-defined colony edge. Morphology of an atypical colony showing signs of differentiation with poorly defined edges and flattened and spreading cells around the periphery, which is characteristic of differentiating cells, is shown in Figure 5B. Figure 5C shows results of manual microdissection of typical colonies where small clumps of cells are cut and used for subculture or harvest.<sup>25,26</sup> This technique allows selection of optimal colonies, and rejection of atypical colonies, for harvest for passage or experiments. This technique minimizes contamination of feeder cells in samples to be analyzed and has been shown to help prevent karyotypic abnormalities.<sup>42</sup> MI01 colonies are composed of 2 cell populations based on laser-light scatter pattern (Figure 5D). Cell-cycle profiles of these 2 different populations can be discerned by flow cytometric dot-plots of laser-light side scatter versus DNA content. To our knowledge, this is the first description of a flow-based technique that allows sorting/analysis of viable cells from these 2 distinct populations within hESC colonies. Figure S6 shows percentages of 2 types of cells from 6 different experiments, demonstrating nearly equal numbers of the 2 cell types. Nocodazole had no significant

influence on this. We refer to the lower population in Figure 5D as hESC-A, and the upper population as hESC-B. A similar analysis of hEB cells derived from MI01 suggests that hESC-As are more similar in pattern to EB cells than are hESC-Bs (Figure 5E). The pluripotent marker protein TRA-1-60<sup>43</sup> was essentially not detected in hESC-As but was abundant in most hESC-Bs, as was SSEA-4<sup>44</sup> (Figure 5F). Most hESC-As were negative for SSEA-4 except for a small number of low-level-expressing cells. OCT-4 expression<sup>45</sup> was observed in hESC-As, but was 10-fold greater in hESC-Bs. These data indicate that hESC-Bs are pluripotent hESCs, while hESC-As are early-differentiated cells. Others have observed heterogeneity in hESC colonies,<sup>12,13</sup> but we believe this is the first demonstration solely using laser-light scatter to identify, quantitate, and analyze them in a way that permits separation of viable cells. Cell-cycle profiles were compared (Figure 5G). The hESC-A control profile was consistent with typical somatic cell cycles, with a pronounced percentage of cells in G<sub>1</sub> phase, while the hESC-B control profile is more typical of ESCs where most are in S phase,<sup>3,46,47</sup> lending further support to the idea of hESC-As being early-differentiated cells and hESC-Bs being pluripotent ESCs. hESC-Bs displayed a native propensity for more than 4C DNA content, although there were no 8C cells. hESC-As clearly show pronounced accumulation of 4C cells after nocodazole treatment and no polyploid cells, in marked contrast to the pattern observed in hESC-Bs showing abundant numbers of 8C cells. These human

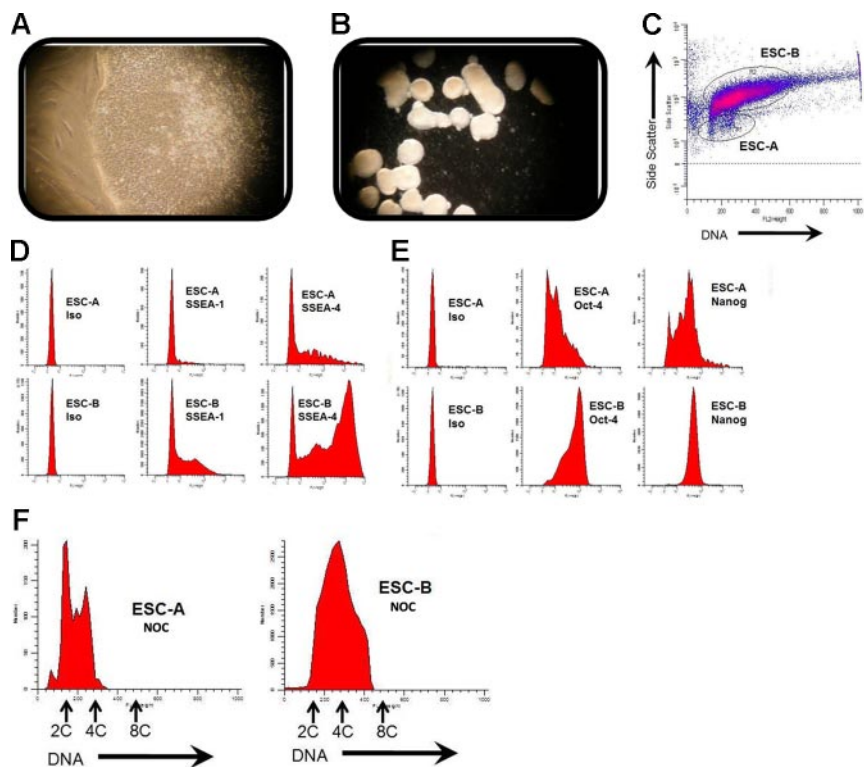


**Figure 6. Colonies of the hESC line HSF-6 also contain 2 populations that differ in marker expression and nocodazole-induced polyploidy.** Colony edge of HSF-6 (A) and hEB (B) formation (Nikon Diaphot; panel A, 10 × 40; panel B, 10 × 20). HSF-6 colonies contain 2 populations based on laser-light scatter pattern (C) analogous to MI01 (Figure 5D). (D-E) Pluripotent marker expression along with nonspecific isotype control antibody binding. HSF-6 colonies were harvested and analyzed as in Figure 5. Cell-cycle analysis of gated hESC-A and hESC-B populations after treatment with nocodazole (F) was done as in Figure 5. Data represent 2 independent experiments.

results are remarkably similar (qualitatively and quantitatively) to those in mESC and mEB cultures (Figures 1-2). Results of 3 experiments with 3 independently thawed and cultured MI01 cells clearly demonstrate generation of polyploid hESC-Bs with absence of polyploid hESC-As after nocodazole treatment (Figure 5H). Figure 6A shows an example of the colony edge and Figure 6B shows the formation of hEBs from another human ESC line, HSF-6. A total of 2 populations were also observed in HSF-6 colonies (Figure 6C), but proportions were different compared with MI01. SSEA-1 and SSEA-4 expression for the A and B populations is shown in Figure 6D and shows that the pluripotent marker SSEA-4 was abundant in hESC-Bs but not in hESC-As. SSEA-1 was negative or low in both populations, suggesting hESC-As are very early in their differentiation program. We also analyzed 2 other pluripotency markers, OCT-4 and nanog. Figure 6E shows that the OCT-4 expression pattern of hESC-As and hESC-Bs was very similar to that of MI01 (Figure 5F), while nanog expression was high in hESC-Bs and lower in hESC-As. Together, the data in Figure 6D and 6E support the idea that hESC-As are early-differentiated cells and hESC-Bs are pluripotent ESCs, analogous to what was observed for the MI01 cell line. Finally, nocodazole treatment of HSF-6 colonies caused more than 4C DNA content in hESC-Bs but not in hESC-As, similar to that observed for MI01. It is noteworthy that prior to our obtaining HSF-6, they were maintained by an enzymatic method of subculture, and it is possible this difference contributed to the less dramatic increase in 8C cells in HSF-6 compared with that in MI01, which has never been subcultured by enzymatic methods. An intrinsic difference between the 2 cell lines, however, cannot be ruled out. This raises the possibility that these 2 culture methods differ in ability to maintain cells in the checkpoint-apoptosis “uncoupled” state. We conclude that pluripotent hESCs, like mESCs, become polyploid (or tolerate/survive the polyploid condition) after checkpoint activation and failed mitosis or aberrant mitotic exit. Differentiated human cells, similar to mEBs, do not become polyploid after

checkpoint activation. These data support the idea that human ESCs are “uncoupled” similarly to mouse ESCs.

## Discussion

We demonstrated 6 salient points: (1) mESCs exit checkpoint-activated mitotic delay and re-enter a polyploid cell cycle; (2) mESCs are resistant to checkpoint-induced apoptosis while ESC-derived mEBs activate robust apoptosis; (3) mESCs tolerate polyploidy and polyploid mitosis for a time in vitro, but decays to near-diploid aneuploidy; (4) when induced to differentiate, polyploid mESCs initiate robust apoptosis and do not form mEBs; (5) differentiation induction, even in the presence of LIF, results in loss of polyploidy-tolerance/survival; also, ectopic suppression of apoptosis in somatic cells results in LIF-independent postcheckpoint polyploidy; and (6) hESC colonies contain 2 distinct populations; pluripotent ESCs and early-differentiated cells. Postcheckpoint polyploidy of these cells is similar to that of mESCs. These points indicate that checkpoint-apoptosis uncoupling is an intrinsic behavior of human and mouse ESCs. The following possibilities are raised: (1) checkpoints are uncoupled from apoptosis in ESCs; (2) early differentiation activates silenced coupling pathways that permit robust apoptotic responses; and (3) karyotypic abnormalities in cultured ESCs may be related to their specialized genome maintenance strategies, including checkpoint-apoptosis uncoupling.

Polyploidy has been observed in mESCs,<sup>48</sup> but mechanisms have not been studied, nor has this behavior been studied in hESCs. We have now defined this process in much greater detail, identified a likely mechanism, and report the first description of nonfusion (mitotic-failure)-induced polyploidy in hESCs. This behavior is in stark contrast to lack of polyploidy tolerance of early-differentiated human cells. Our data suggests that the switch from uncoupling/polyploidy tolerance to coupling/polyploidy intolerance occurs very early upon initiation of differentiation programs and may

coincide with lineage specification and loss of “stem-like” self-renewal. The novel concept of checkpoint-apoptosis uncoupling in pluripotent stem cells, as opposed to the concept that the checkpoint itself is nonfunctional, may also be applicable to other checkpoints that activate apoptosis, such as the DNA damage checkpoint.<sup>4,49</sup> Others<sup>50-53</sup> have shown mouse and human ESCs tolerate chemical fusion-induced tetraploidy, a technique used to generate ESC-specific cloned animals (tetraploid-embryo complementation). This technique (chemical fusion) has also been used to demonstrate reprogramming of somatic genomes into embryonic-like genomes;<sup>54</sup> cultures containing tetraploid (somatic/ESC) hybrid cells formed teratomas composed of cells representing 3 germ layers after injection into mice, indicating the hybrids were pluripotent. This is an important step toward full use of ESC technology for human benefit. However, our data indicates that polyploid ESCs can reduce their ploidy to near-diploid aneuploidy after short times in culture, thus raising the possibility that teratoma formed from hybrid cells may be derived from near-diploid/aneuploid ESCs instead of complete tetraploids, especially since evidence demonstrating tetraploidy in the hybrid-derived teratoma cells is lacking. It is reported that chemical fusion-induced tetraploid ESCs display a decay/reduction in chromosome number during culture, similar to our findings. Unequal segregation of chromosomes and even a degree of chromosome selectivity in this process favoring the embryonic chromosomes (ie, loss of somatic chromosomes) has been reported.<sup>51</sup> It is therefore possible that the complete somatic genome contingent of somatic/ESC hybrid cells may not be represented in the teratoma cells, and this might lead to false impressions of genome reprogramming.

Our findings are consistent with Stewart et al,<sup>55</sup> who reported cellular heterogeneity in hESC colonies. They observed differences in cell-cycle behavior between SSEA3<sup>+</sup> and SSEA3<sup>-</sup> cells in the same colonies, similar to types A and B cell populations we observed in hESC colonies (Figures 5-6) using markers SSEA1, SSEA4, TRA-1-60, Oct-4, and nanog. Our hESC-A and -B cells may be similar, if not identical, to SSEA3<sup>+/+</sup> cells.<sup>55</sup> It is likely that the SSEA1-Hi/Lo mESC populations (Figure 4C) are murine analogs to the 2 human cell types. Our data and those of Stewart et al are consistent with a very narrowly defined phenotypic switch from very primitive ESC-like behavior to less primitive progenitor cell-like behavior. It is interesting that this apparently abrupt shift in phenotype in both studies is characterized by a marked and specific shift in cell-cycle behavior. This is reminiscent of the abrupt shift in cell-cycle behavior at the midblastula transition in amphibian and starfish embryos, where the G<sub>1</sub> phase is greatly lengthened asynchronously.<sup>56</sup> Our data suggest that checkpoint-apoptosis coupling may be another determinant characterizing 1 of the earliest changes from pluripotency/self-renewal (ESC-like) to differentiation/lineage commitment (progenitor cell-like).

Another issue highlighted by our data is the interpretations of checkpoint deficiency or absence in ESCs.<sup>57</sup> Many techniques to measure and quantify checkpoint integrity often rely on proper function of other checkpoints like the SAC. Because our data suggest the SAC is functional in ESCs but does not conform to conventional concepts (ie, uncoupling), it is possible to be misled by data where the SAC is assumed to behave as in somatic cells. The decatenation checkpoint is reported to be deficient in mESCs and neural and hematopoietic progenitor cells.<sup>57</sup> Because the technique used to quantitate function of this checkpoint (pseudomitotic index) relies on accumulation of cells in metaphase by treatment with spindle inhibitors like colchicine or nocodazole, and results are expressed as a ratio of frequency of pseudomitotic cells

(cells that have entangled but condensed chromosomes) versus frequency of normal mitotic cells (normally condensed chromosomes), results can be influenced not only by changes in pseudomitotic cell numbers, but also by changes in normal mitotic cell numbers. Our data suggest that the frequency of normal mitotic cells observed after treatment with spindle poisons, like colchicine, may not accurately reflect the numbers of cells that have entered and exited mitosis in mESCs compared with differentiated cells. Thus, an alternative interpretation of the reported pseudomitotic index data<sup>57</sup> is that the SAC, and not necessarily the decatenation checkpoint, is deficient. We observed low numbers of apparent pseudomitotic cells in mESCs after short treatment times (6-10 hours), but they were not quantitated (data not shown). Our data are thus consistent with previous reports of an apparent deficient decatenation checkpoint in mESCs compared with mEBs.

Based on findings of increased pseudomitotic index in neural and hematopoietic progenitor cells<sup>57</sup> and our data, we hypothesize that tissue-specific stem/progenitor cells may also be characterized by lack of SAC-apoptosis coupling. This may have implications for techniques to culture and expand, *ex vivo*, adult stem cells and primary progenitor cells. Rigorous examination of SAC function in populations of primary mouse *scal<sup>1</sup>/lin<sup>-</sup>/c-kit<sup>+</sup>* and human CD34<sup>+</sup>/CD38<sup>-</sup> cells, highly enriched in primitive hematopoietic progenitors, could be used to test this hypothesis. The physiologic relevance of checkpoint-apoptosis uncoupling in tissue-specific progenitors is unknown, but is likely important for strategies to maintain genomic integrity and tumor suppression in progenitors as it appears to be for ESCs.

Our studies lead to the question why ESCs would maintain corrupted/genome-damaged cells, and what advantage this behavior might have during early embryogenesis. One possibility is that in early developing embryos, a cell, even though it may be genetically corrupt, can still maintain a supportive role for initial patterning and asymmetry generation via lateral-inhibition and morphogen-diffusion/gradient formation,<sup>58</sup> and might be important for early embryo survival when cell numbers are low. Only later, after initial patterning and sufficient “cell mass” is achieved such that loss of some cells via apoptotic culling of damaged cells can be tolerated without disruption of overall patterning, would surveillance and culling become safely activated. This could be why checkpoint-apoptosis uncoupling might exist in very early developing embryos, especially for caspase-dependent apoptosis, which is context dependent in mammals and related to stress/damaging agent or tissue type and is highly dependent on developmental status.<sup>58</sup> If this notion is correct, then when ESCs are removed from the context of early embryonic development in the preimplantation blastocyst and immortalized in culture, they could remain uncoupled and subject to increased genome damage. If this is so, it should lead to new strategies to help maintain genomic fidelity in ESC cultures.

Finally, our studies suggest that links between karyotypic instability in stem cells and notions of a “cancer stem cell”<sup>59</sup> may be partly founded in the propensity of ESCs, and potentially adult stem cells,<sup>57</sup> to suffer from intrinsic checkpoint-apoptosis uncoupling. A Lats2-Mdm2-p53 axis checkpoint has recently been described in somatic cells,<sup>60</sup> which is critical for maintenance of proper chromosomal segregation after mitotic slippage due to dysfunction of the mitotic spindle apparatus. Better understanding of this process is lacking and this has not yet been evaluated in mESCs. p53 down-regulates nanog expression,<sup>61</sup> which maintains self-renewal/pluripotency in ESCs.



We recently found that the histone-deacetylase SIRT1 (which has p53 as one of its substrates), is required for proper p53 nuclear translocation and nanog down-regulation<sup>61</sup> (M.K.H., Y.G., X.O., C.M., and H.E.B., unpublished observations, November 2006). p53 and SIRT1 are highly expressed in mESCs, but p53 is believed to be in a nonfunctional form in mESCs (M.K.H., Y.G., X.O., C.M., and H.E.B., unpublished observations, November 2006), which could be explained by SIRT1 maintaining p53 in a deacetylated (cytoplasmic) form, which is unable to activate apoptosis-related genes or down-regulate nanog. In somatic cells, SIRT1 is very low, permitting access of p53 into the nucleus to activate its proapoptotic function, down-regulate nanog, and initiate differentiation, where p53 would behave as it is known to do in somatic cells. These ideas are highly speculative at this time.

Understanding molecular mechanisms of checkpoint-apoptosis coupling/uncoupling in ESCs and adult stem cells and their differentiated derivatives could provide important clues about chromosomal instability (CIN) in human tumors,<sup>62</sup> as well as provide new ways to exploit this behavior for therapeutic benefit.

## Acknowledgments

We thank P. Mantel for editing the manuscript; B. Graham, Mee-Young Cho, and Kyu-Yong Han for helpful discussions; and S. Rhorabough and C. Kaufman for superb technical support.

## References

- Huppertz B, Herrler A. Regulation of proliferation and apoptosis during development of the preimplantation embryo and the placenta. *Birth Defects Res C Embryo Today*. 2005;75:249-261.
- Jefford CE, Irminger-Finger I. Mechanisms of chromosome instability in cancers. *Crit Rev Oncol Hematol*. 2006;59:1-14.
- Burdon T, Smith A, Savatier P. Signalling, cell cycle and pluripotency in embryonic stem cells. *Trends Cell Biol*. 2002;12:432-438.
- Holway AH, Kim SH, La Volpe A, Michael WM. Checkpoint silencing during the DNA damage response in *Caenorhabditis elegans* embryos. *J Cell Biol*. 2006;172:999-1008.
- Fluckiger AC, Marcy G, Marchand M, et al. Cell cycle features of primate embryonic stem cells. *Stem Cells*. 2006;24:547-556.
- Pampfer S, Donnay I. Apoptosis at the time of embryo implantation in mouse and rat. *Cell Death Differ*. 1999;6:533-545.
- Spanos S, Rice S, Karagiannis P, et al. Caspase activity and expression of cell death genes during development of human preimplantation embryos. *Reproduction*. 2002;124:353-363.
- Duval D, Trouillas M, Thibault C, et al. Apoptosis and differentiation commitment: novel insights revealed by gene profiling studies in mouse embryonic stem cells. *Cell Death Differ*. 2006;13:564-575.
- Wells D, Bermudez MG, Steuerwald N, et al. Expression of genes regulating chromosome segregation, the cell cycle and apoptosis during human preimplantation development. *Hum Reprod*. 2005;20:1339-1348.
- Greenwood J, Costanzo V, Robertson K, Hensley C, Gautier J. Responses to DNA damage in *Xenopus*: cell death or cell cycle arrest. *Novartis Found Symp*. 2001;237:221-230.
- Greenwood J, Gautier J. From oogenesis through gastrulation: developmental regulation of apoptosis. *Semin Cell Dev Biol*. 2005;16:215-224.
- Semb H. Human embryonic stem cells: origin, properties and applications. *APMIS*. 2005;113:743-750.
- Edwards RG. Stem cells today, A: origin and potential of embryo stem cells. *Reprod Biomed Online*. 2004;8:275-306.
- Longo L, Bygrave A, Grosveld FG, Pandolfi PP. The chromosome make-up of mouse embryonic stem cells is predictive of somatic and germ cell chimaerism. *Transgenic Res*. 1997;6:321-328.
- Humpherys D, Eggan K, Akutsu H, et al. Epigenetic instability in ES cells and cloned mice. *Science*. 2001;293:95-97.
- Humpherys D, Eggan K, Akutsu H, et al. Abnormal gene expression in cloned mice derived from embryonic stem cell and cumulus cell nuclei. *Proc Natl Acad Sci U S A*. 2002;99:12889-12894.
- Cervantes RB, Stringer JR, Shao C, Tischfield JA, Stambrook PJ. Embryonic stem cells and somatic cells differ in mutation frequency and type. *Proc Natl Acad Sci U S A*. 2002;99:3586-3590.
- Pera MF. Unnatural selection of cultured human ES cells? *Nat Biotechnol*. 2004;22:42-43.
- Draper JS, Moore HD, Ruban LN, Gokhale PJ, Andrews PW. Culture and characterization of human embryonic stem cells. *Stem Cells Dev*. 2004;13:325-336.
- Draper JS, Smith K, Gokhale P, et al. Recurrent gain of chromosomes 17q and 12 in cultured human embryonic stem cells. *Nat Biotechnol*. 2004;22:53-54.
- Eggan K, Rode A, Jentsch I, et al. Male and female mice derived from the same embryonic stem cell clone by tetraploid embryo complementation. *Nat Biotechnol*. 2002;20:455-459.
- Guo Y, Costa R, Ramsey H, et al. The embryonic stem cell transcription factors Oct-4 and FoxD3 interact to regulate endodermal-specific promoter expression. *Proc Natl Acad Sci U S A*. 2002;99:3663-3667.
- Guo Y, Graham-Evans B, Broxmeyer HE. Murine embryonic stem cells secrete cytokines/growth modulators that enhance cell survival/anti-apoptosis and stimulate colony formation of murine hematopoietic progenitor cells. *Stem Cells*. 2006;24:850-856.
- National Institutes of Health Human Stem Cell Registry. <http://stemcells.nih.gov/research/registry.html>. Accessed December 12, 2005.
- Suh MR, Lee Y, Kim JY, et al. Human embryonic stem cells express a unique set of microRNAs. *Dev Biol*. 2004;270:488-498.
- Lee JB, Lee JE, Park JH, et al. Establishment and maintenance of human embryonic stem cell lines on human feeder cells derived from uterine endometrium under serum-free condition. *Biol Reprod*. 2005;72:42-49.
- Mantel C, Braun SE, Reid S, et al. p21(cip-1/waf-1) deficiency causes deformed nuclear architecture, centriole overduplication, polyploidy, and relaxed microtubule damage checkpoints in human hematopoietic cells. *Blood*. 1999;93:1390-1398.
- Shibayama H, Takai E, Matsumura I, et al. Identification of a cytokine-induced antiapoptotic molecule anamorsin essential for definitive hematopoiesis. *J Exp Med*. 2004;199:581-592.
- Fukuda S, Mantel CR, Pelus LM. Survivin regulates hematopoietic progenitor cell proliferation through p21WAF1/Cip1-dependent and -independent pathways. *Blood*. 2004;103:120-127.
- Mantel CR, Braun SE, Lee Y, Kim YJ, Broxmeyer HE. The interphase microtubule damage checkpoint defines an S-phase commitment point and does not require p21(waf-1). *Blood*. 2001;97:1505-1507.
- Bagwell CB. Hyperlog-a flexible log-like transform for negative, zero, and positive valued data. *Cytometry A*. 2005;64:34-42.
- Henegariu O, Heerema NA, Bray-Ward P, Ward DC. Colour-changing karyotyping: an alternative to M-FISH/SKY. *Nat Genet*. 1999;23:263-264.
- Henegariu O, Heerema NA, Lowe Wright L, Bray-Ward P, Ward DC, Vance GH. Improvements in cytogenetic slide preparation: controlled chromosome spreading, chemical aging and gradual denaturing. *Cytometry*. 2001;43:101-109.
- Lanni JS, Jacks T. Characterization of the p53-dependent postmitotic checkpoint following

This work was supported by US Public Health Service Grants R01 HL67384, a supplement to HL67384, R01 HL56416, a Project in P01 HL053586 (H.E.B.), and R01 HL79654 and R01 HL69669 (L.M.P.), and a grant (SC2060) from the Stem Cell Research Center of the 21st Century Frontier Research Program and the Ministry of Science and Technology, Republic of Korea (K.-S.K.).

## Authorship

Contribution: C.M. designed and performed research, collected and analyzed data, and cowrote the paper. Y.G. designed research; M.R.L., M.-K.K., and M.-K.H. performed difficult but vital cell line culture and designed research; H.S. contributed vital reagents and cell lines; S.F., M.C.Y., and L.M.P. contributed vital cell lines; K.-S.K. supported the study, contributed vital cell lines and reagents, and analyzed the data; and H.E.B. supported the study, analyzed data, and cowrote the paper.

Conflict-of-interest statement: All authors declare no competing financial interests.

Correspondence: Hal E. Broxmeyer or Charlie R. Mantel, Walther Oncology Center, Indiana University School of Medicine, Room 302A, 950 West Walnut St, Indianapolis, IN 46202; e-mail: hbroxmey@iupui.edu or cmantel@iupui.edu; or Kye-Seong Kim, Department of Anatomy and Cell Biology, Hanyang University College of Medicine, Seoul, Korea; e-mail: ks66kim@hanyang.ac.kr.

- spindle disruption. *Mol Cell Biol*. 1998;18:1055-1064.
35. Lanni JS, Lowe SW, Licitra EJ, Liu JO, Jacks T. p53-independent apoptosis induced by paclitaxel through an indirect mechanism. *Proc Natl Acad Sci U S A*. 1997;94:9679-9683.
  36. Sanchez-Aguilera A, Montalban C, de la Cueva P, et al. Tumor microenvironment and mitotic checkpoint are key factors in the outcome of classical Hodgkin lymphoma. *Blood*. 2006;108:662-668.
  37. Andrews PW, Goodfellow PN. Antigen expression by somatic cell hybrids of a murine embryonal carcinoma cell with thymocytes and L cells. *Somatic Cell Genet*. 1980;6:271-284.
  38. Borel F, Lohez OD, Lacroix FB, Margolis RL. Multiple centrosomes arise from tetraploidy checkpoint failure and mitotic centrosome clusters in p53 and RB pocket protein-compromised cells. *Proc Natl Acad Sci U S A*. 2002;99:9819-9824.
  39. Pozarowski P, Huang X, Halicka DH, Lee B, Johnson G, Darzynkiewicz Z. Interactions of fluorochrome-labeled caspase inhibitors with apoptotic cells: a caution in data interpretation. *Cytometry A*. 2003;55:50-60.
  40. Darzynkiewicz Z, Bedner E. Analysis of apoptotic cells by flow and laser scanning cytometry. *Methods Enzymol*. 2000;322:18-39.
  41. van Engeland M, Nieland LJ, Ramaekers FC, Schutte B, Reutelingsperger CP. Annexin V-affinity assay: a review on an apoptosis detection system based on phosphatidylserine exposure. *Cytometry*. 1998;31:1-9.
  42. Mitalipova MM, Rao RR, Hoyer DM, et al. Preserving the genetic integrity of human embryonic stem cells. *Nat Biotechnol*. 2005;23:19-20.
  43. Andrews PW, Banting G, Damjanov I, Arnaud D, Avner P. Three monoclonal antibodies defining distinct differentiation antigens associated with different high molecular weight polypeptides on the surface of human embryonal carcinoma cells. *Hybridoma*. 1984;3:347-361.
  44. Kannagi R, Cochran NA, Ishigami F, et al. Stage-specific embryonic antigens (SSEA-3 and -4) are epitopes of a unique globo-series ganglioside isolated from human teratocarcinoma cells. *EMBO J*. 1983;2:2355-2361.
  45. Brehm A, Ovitt CE, Scholer HR. Oct-4: more than just a POUerful marker of the mammalian germline? *APMIS*. 1998;106:114-124.
  46. Artus J, Babinet C, Cohen-Tannoudji M. The cell cycle of early mammalian embryos: lessons from genetic mouse models. *Cell Cycle*. 2006;5:499-502.
  47. Fujii-Yamamoto H, Kim JM, Arai K, Masai H. Cell cycle and developmental regulations of replication factors in mouse embryonic stem cells. *J Biol Chem*. 2005;280:12976-12987.
  48. Malashicheva AB, Kisliakova TV, Savatier P, Pospelov VA. [Embryonal stem cells do not undergo cell cycle arrest upon exposure to damaging factors]. *Tsitologiia*. 2002;44:643-648.
  49. Aladjem MI, Spike BT, Rodewald LW, et al. ES cells do not activate p53-dependent stress responses and undergo p53-independent apoptosis in response to DNA damage. *Curr Biol*. 1998;8:145-155.
  50. Nagy A, Rossant J, Nagy R, Abramow-Newerly W, Roder JC. Derivation of completely cell culture-derived mice from early-passage embryonic stem cells. *Proc Natl Acad Sci U S A*. 1993;90:8424-8428.
  51. Matveeva NM, Pristyazhnyuk IE, Temirova SA, et al. Unequal segregation of parental chromosomes in embryonic stem cell hybrids. *Mol Reprod Dev*. 2005;71:305-314.
  52. Li X, Wei W, Yong J, Jia Q, Yu Y, Di K. The genetic heterozygosity and fitness of tetraploid embryos and embryonic stem cells are crucial parameters influencing survival of mice derived from embryonic stem cells by tetraploid embryo aggregation. *Reproduction*. 2005;130:53-59.
  53. Li X, Wei W, Yong J, Jia Q, Yu Y, Di K. The genetic heterozygosity and fitness of tetraploid embryos and embryonic stem cells are crucial parameters influencing survival of mice derived from embryonic stem cells by tetraploid embryo aggregation. *Reproduction*. 2005;130:53-59.
  54. Cowan CA, Atienza J, Melton DA, Eggan K. Nuclear reprogramming of somatic cells after fusion with human embryonic stem cells. *Science*. 2005;309:1369-1373.
  55. Stewart MH, Bosse J, Chadwick K, Menendez P, Bendall SC, Bhatia M. Clonal isolation of hESCs reveals heterogeneity within the pluripotent stem cell compartment. *Nat Methods*. 2006;3:807-815.
  56. Etkin LD. Regulation of the mid-blastula transition in amphibians. *Dev Biol (N Y)* 1985). 1988;5:209-225.
  57. Damelin M, Sun YE, Sodja VB, Bestor TH. Decatenation checkpoint deficiency in stem and progenitor cells. *Cancer Cell*. 2005;8:479-484.
  58. Gurdon JB, Bourillot PY. Morphogen gradient interpretation. *Nature*. 2001;413:797-803.
  59. Zhang M, Rosen JM. Stem cells in the etiology and treatment of cancer. *Curr Opin Genet Dev*. 2006;16:60-64.
  60. Aylon Y, Michael D, Shmueli A, Yabuta N, Nojima H, Oren M. A positive feedback loop between the p53 and Lats2 tumor suppressors prevents tetraploidization. *Genes Dev*. 2006;20:2687-2700.
  61. Lin T, Chao C, Saito S, et al. p53 induces differentiation of mouse embryonic stem cells by suppressing Nanog expression. *Nat Cell Biol*. 2005;7:165-171.
  62. Lengauer C, Kinzler KW, Vogelstein B. Genetic instabilities in human cancers. *Nature*. 1998;396:643-649.